

---

# Tropical-Ocean--Atmosphere Interactions in a Coupled Model [and Discussion]

C. Gordon and J. D. Neelin

*Phil. Trans. R. Soc. Lond. A* 1989 **329**, 207-223  
doi: 10.1098/rsta.1989.0071

---

## Email alerting service

Receive free email alerts when new articles cite this article - sign up in the box at the top right-hand corner of the article or click [here](#)

---

To subscribe to *Phil. Trans. R. Soc. Lond. A* go to: <http://rsta.royalsocietypublishing.org/subscriptions>

---

## Tropical-ocean–atmosphere interactions in a coupled model

BY C. GORDON

*Meteorological Office Unit, Hooke Institute for Atmospheric Research, Clarendon Laboratory,  
University of Oxford, Parks Road, Oxford OX1 3PU, U.K.*

A high-resolution tropical Pacific Ocean model coupled to a medium-resolution atmospheric general circulation model has been integrated for  $2\frac{1}{2}$  years. A seasonal cycle was included. The atmospheric model when forced with climatological seasonally varying sea surface temperatures simulates the surface stress and net surface heating over the tropical Pacific Ocean to within the uncertainty in the climatological estimates in these quantities. When coupled, however, the models drift into an annually recurring anomalous state, similar in many respects to the El Niño Southern Oscillation observed in the ocean and atmosphere. The model results emphasize the role of off-equatorial anomalies in temperature, atmospheric heating and wind response. Air–sea heat exchange is found to be dominant in determining sea surface temperature changes in these off-equatorial regions. Both cloud and evaporative feedbacks are important in the anomalous surface heat budget.

### 1. INTRODUCTION

The aim in developing general circulation models (GCMs) of the tropical-Pacific-Ocean–global-atmosphere is both to provide a forecasting tool and to investigate the physical mechanisms and instabilities at play within the coupled system. Simple models of the coupled system already exist and have shown skill in their ability to forecast broad features of El Niño events (Cane *et al.* 1986). The essential difference between the simple models and the GCMs is the limited range of physical interactions in the former compared with the latter. This does not mean, necessarily, that the GCMs are more realistic but they clearly have the potential to be so. If feedbacks can be identified within a coupled GCM simulation that is realistic in terms of the quantities that can be measured (for example sea surface temperature (SST), low-level winds, etc.) then these feedbacks may well be important in the real ocean–atmosphere system. These coupled models should also be capable of providing a detailed description of the evolution of an anomalous event and such information is clearly of importance.

There are good reasons to believe that a coupled GCM of the tropical-ocean–global-atmosphere (TOGA) system can realistically simulate many of the interactions occurring during an El Niño Southern Oscillation (ENSO) event. The success of atmospheric models in simulating the major tropical response to SST anomalies is encouraging (Shukla & Blackmon 1986). The parallel success of ocean GCMs, forced with estimates of wind stress for 1982–83, in simulating many of the major oceanographic features of the 1982–83 El Niño is another reason for optimism (Philander & Seigel 1985). Taken together, the apparent realism of both component models suggests that coupled together such models might be capable of providing a reasonable simulation of the ocean–atmosphere system.

Of particular relevance to the coupled interactions are model simulations of variables at the air–sea interface, namely the SST and the surface fluxes of momentum, heat and fresh water. In

practice, ocean models have particular difficulty in simulating SST and atmospheric models in simulating surface fluxes; see von Storch *et al.*; Cubasch; Gilchrist (all this Symposium). The reasons for this are not hard to find. The SST depends on many processes within the ocean, as well as on the atmospheric forcing itself, whereas the surface fluxes depend on many, often sub-grid scale, processes in the atmosphere. A problem also encountered is the lack of accurate observational estimates of the surface fluxes over the ocean both to force ocean models and verify atmospheric model fluxes. This would not be important if the ocean models were not sensitive at the level of uncertainty in these fluxes. This, however, is not the case and uncoupled ocean experiments with different flux products have shown the ocean GCMs to be very sensitive, especially in the SST response, to the differences in these forcing fields (Gordon & Corry 1989). Although this will not be discussed in detail, we note here that the fluxes of momentum and heat from the atmospheric model employed in the simulations described below are within the (considerable) uncertainties in the existing climatological estimates of these quantities.

The combined effect of the limitations of both ocean and atmosphere models in simulating the variables at the air-sea interface tends to lead to a 'climate drift' within the coupled system. This also happens in the component models when integrated alone. In an attempt to eliminate the effects of climate drift from a climate perturbation experiment the procedure of performing a 'control' integration as well as the perturbed anomaly experiment is usually adopted. The model response to anomalous forcing is then determined by differencing the anomaly model response with that from the control simulation. In SST anomaly experiments the anomalous response in a given model has been found to depend significantly on the control climate simulation of the model (Mansfield & Palmer 1986). This is also likely to be the case in coupled model simulations although the situation is further complicated by the systematic errors associated with the ocean model. An approach has been developed (von Storch and Cubasch, this symposium), known as flux correction, to artificially remove the climate drift effects from the surface variables but this has not been used in the simulation described in this paper.

The results described below are from a control integration of a coupled model. It turns out that the drift in this model exhibits many features similar to those associated with ENSO episodes. Despite the origins of these features the SST simulation is quite realistic and the feedbacks occurring within the model may well take place in the real coupled system.

## 2. THE COUPLED MODEL

The global atmospheric component of the coupled model is a version of the British Meteorological Office eleven-layer climate model on a  $2.5^\circ \times 3.75^\circ$  latitude-longitude grid (Slingo *et al.* 1989). The model includes a detailed representation of boundary layer and surface processes, interactive radiation and cloud and a parametrization of penetrative convection. An additional parametrization of the effects of sub-grid scale gustiness, associated with vigorous convection, on the surface heat and momentum fluxes was also included in the version of the model used in the coupled experiment. Data from the GATE B-scale array was used to relate a measure of surface wind gustiness to the precipitation rate and this relation was then used in the GCM.

The ocean model is a high-resolution version of the model described by Cox (1984). The domain is the tropical Pacific between  $30^\circ$  N and  $30^\circ$  S and SSTs outside this region are updated with seasonally varying climatological values. The boundary conditions at  $30^\circ$  N and

30° S are chosen to ensure a smooth transition between the predicted temperatures within the ocean model domain and the climatological temperatures specified outside. The ocean model has a non-uniform grid resolution with a 0.33° spacing on the Equator and 0.5° at the meridional boundaries. The lowest resolution occurs in the central Pacific near the zonal boundaries where the grid spacing is 1.5° and 1° in the zonal and meridional directions respectively. There is a 10 m vertical resolution near to the ocean surface and the K-theory mixing scheme of Pacanowski & Philander (1981) is used to parametrize vertical turbulent transports. The ocean model has an active salinity field.

Both the atmosphere and ocean components have been used extensively as independent models. Various versions of the atmospheric model have been integrated both with seasonally varying SSTs (Slingo *et al.* 1989) and with anomalous SSTs in both tropical and extra-tropical regions (Mansfield & Palmer 1986). The ocean model has been used to simulate the seasonal cycle by using a number of surface forcing products and also to simulate the evolution of the 1982–83 El Niño (Gordon & Corry 1989). When coupled, the surface fluxes are accumulated each timestep in the atmospheric model and average values passed to the ocean model every five days. The ocean model is then integrated for five days with these fluxes and the resulting SST distribution passed back to the atmospheric model.

The initial ocean state for the coupled simulations was prepared by spinning up the ocean model for four years with the atmospheric GCM surface wind stresses derived from a long integration of the atmospheric model with climatological (seasonally varying) sea surface temperatures. This was done to minimize the initial imbalance between the equatorial zonal pressure gradient in the thermocline and the surface stress. Such an imbalance may lead to the generation of a spurious El Niño-like event in the ocean model. The coupled model integration was begun at a time corresponding to the beginning of July and was integrated for 31 months. The initial state is not specific to a particular phase of the ENSO cycle, for example, to pre-El Niño conditions. This does not rule out the possibility that, inadvertently, the initial state is primed in a way that is favourable to ENSO but the indications from the 2½ year experiment are that the ocean response is being repeated each year as part of the model seasonal cycle and is not determined primarily by the initial conditions.

### 3. RESULTS

The tropical Pacific climatological SST distributions for March and September from the British Meteorological Office analyses (Bottomley *et al.* 1989) are shown in figures 1*a* and 2*a*. These months represent the two extremes of the seasonal cycle. In September the warm pool is situated in the Northern Hemisphere and the east Pacific cold tongue is near to its maximum extension (figure 2*a*). In March the warm pool has moved with the sun to the Southern Hemisphere and is situated under the South Pacific Convergence Zone (SPCZ). In the east the cold tongue is near its minimum extension (figure 1*a*). The seasonal cycle in the west is most likely caused by the seasonal variations in local heating whereas in the east, upwelling, advection and local effects may all be important. The coupled model simulation of SST for March and September, from the first two years of the integration, are depicted in figures 1*b, c* and 2*b, c* respectively. The simulation for each of these months will be discussed in turn and the atmospheric response compared with that obtained from a parallel integration of the atmospheric model with seasonally varying climatological SSTs.

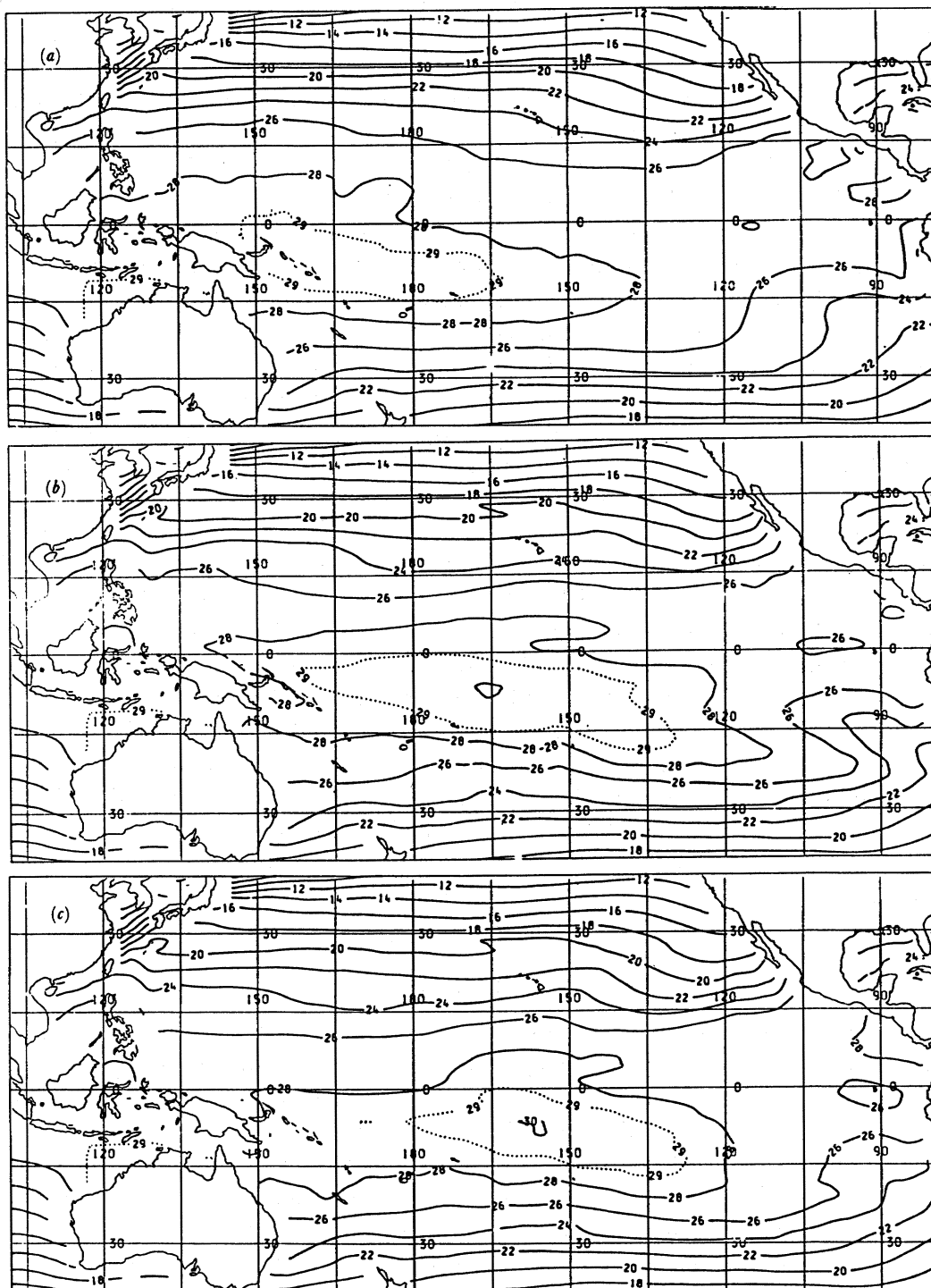


FIGURE 1. Monthly mean SST for March from (a) U.K. Meteorological Office climatology, (b) the first March in the coupled integration, (c) the second March in the coupled integration. In both years in the coupled simulation the warm pool is shifted from the west into the central Pacific. The contour interval is 2 °C with an additional (broken) 29 °C contour.



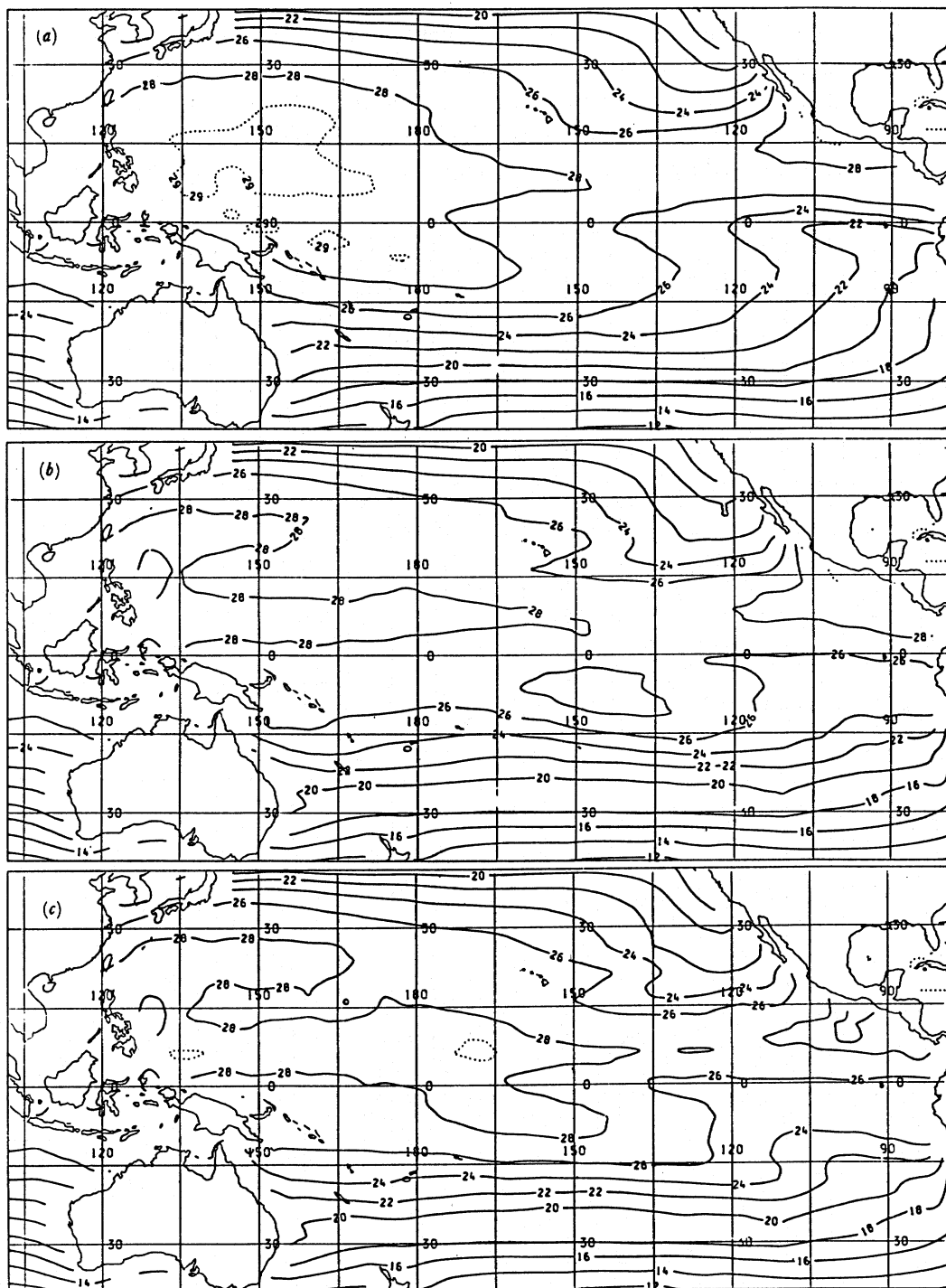


FIGURE 2. As figure 1 but for September. There is no west Pacific warm pool north of the equator in the coupled model. The maximum SSTs are situated east of the dateline in the Inter Tropical Convergence Zone.

*(a) March*

It is evident from the coupled model March SST fields for each year that they are more similar to each other than to the climatological distribution in figure 1*a*. The warm pool is situated too far east and is separated from the coast, a situation more characteristic of recent El Niño events than of climatology. The significance of this shift in position of the warm pool on the atmosphere can be assessed by comparing the 250 mbar† velocity potential and divergent wind

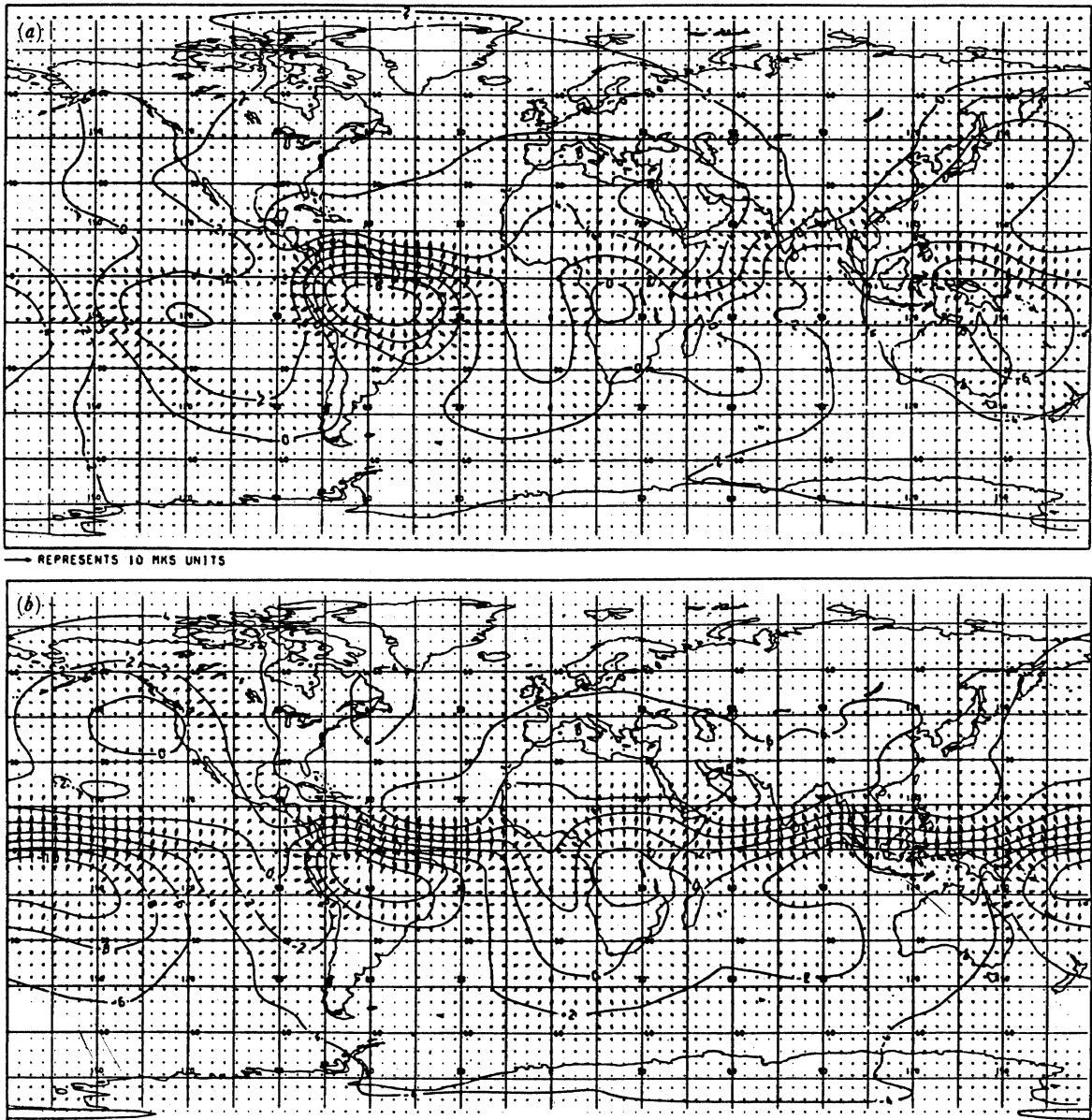


FIGURE 3. The March velocity potential and divergent wind at 250 mbar as simulated by the atmospheric model in (a) a simulation with climatological seasonally varying SSTs and (b) the first year of the coupled experiment. In the coupled simulation the main Pacific forcing region is moved from its climatological position over the New Guinea–northeast Australia region, to lie over the warmest water east of the dateline.

† 1 mbar =  $10^2$  Pa.

fields for March shown in figure 3. Figure 3*a* is taken from the atmospheric model integration with climatologically varying SSTs and figure 3*b* from the second March of the coupled simulation. In association with the anomalous warm pool of water in the central Pacific of the coupled model the main atmospheric forcing region moves eastwards to be situated over the warmest water (figure 3*b*). The model atmosphere wind response near the surface is illustrated by the wind stress fields given in figure 4. Figure 4*a* is a March stress field from the control integration and figure 4*b* the equivalent field from the second March of the coupled experiment. The stresses in figure 4*a* are quite reasonable when compared with existing climatologies for the tropical Pacific, with the major deficiency being the large stress gradients to the north of the Inter Tropical Convergence Zone (ITCZ). Both figure 4*a* and *b* are from a single month in GCM integrations so the natural atmospheric variability, especially in the

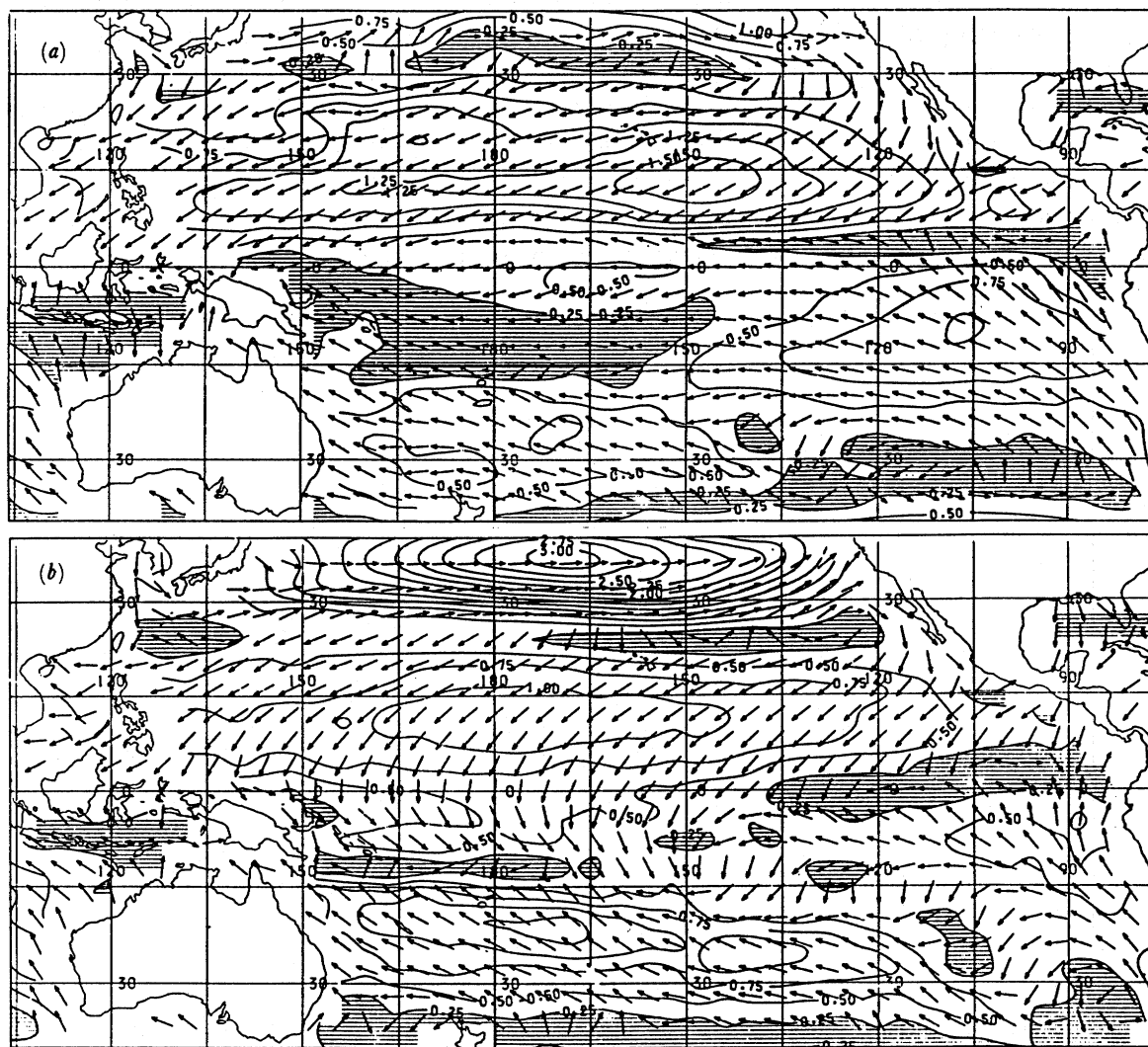


FIGURE 4. The March surface wind stress as simulated by the atmospheric model in (a) a simulation with climatological seasonally varying SSTs and (b) the first year of the coupled experiment. The stress field produced with climatological SSTs is a reasonable realization compared to climatological estimates. The stress from the coupled model shows flow into the anomalous forcing region and northerly flow across the equator in the west equatorial Pacific. The contour interval is  $0.25 \text{ dyn cm}^{-2}$  and areas with stresses less than  $0.25 \text{ dyn cm}^{-2}$  are shaded, where  $1 \text{ dyn} = 10^{-5} \text{ N}$ . (Arrows show direction only.)



trades, must be born in mind when comparing these. It is evident, however, that there are fundamental differences in the coupled model response. It can be seen from figure 4*b* that from 135° E to 165° W there is northerly flow across the Equator whereas, by contrast, the stresses in this region in figure 4*a* (and climatology) are largely zonal. This anomalous low-level flow in the coupled model is being forced by the anomalous SST distribution. It is interesting that the removal of the zonal wind stress component in the equatorial regions, which is forced by the off-equatorial warming, will lead to a reduction in upwelling and rise in SST on the Equator, as can be seen in figure 2*b, c*. Another feature of note in the coupled model stress field is the reduction in strength of the southeast trades (in the simulation there is also a reduction and southward shift in the position of the south Pacific high).

To investigate the coupled model response in greater detail, various model variables were averaged over a region from approximately 2.5–15° S and 180–135° W. This region corresponds to the area occupied by the anomalously warm water for much of the year. The SST evolution in this region from both climatology and the model is shown in figure 5. The too-warm model temperatures in the Southern Hemisphere summer are seen to follow a regular cycle each year. Even though the mean temperature error is less than 1 °C this turns out to be very significant. The corresponding convective precipitation rates calculated in the atmospheric model control integration and the coupled simulation are shown in figure 7. There is a large increase in precipitation in the coupled model in association with the warmer SST. The latent heat release

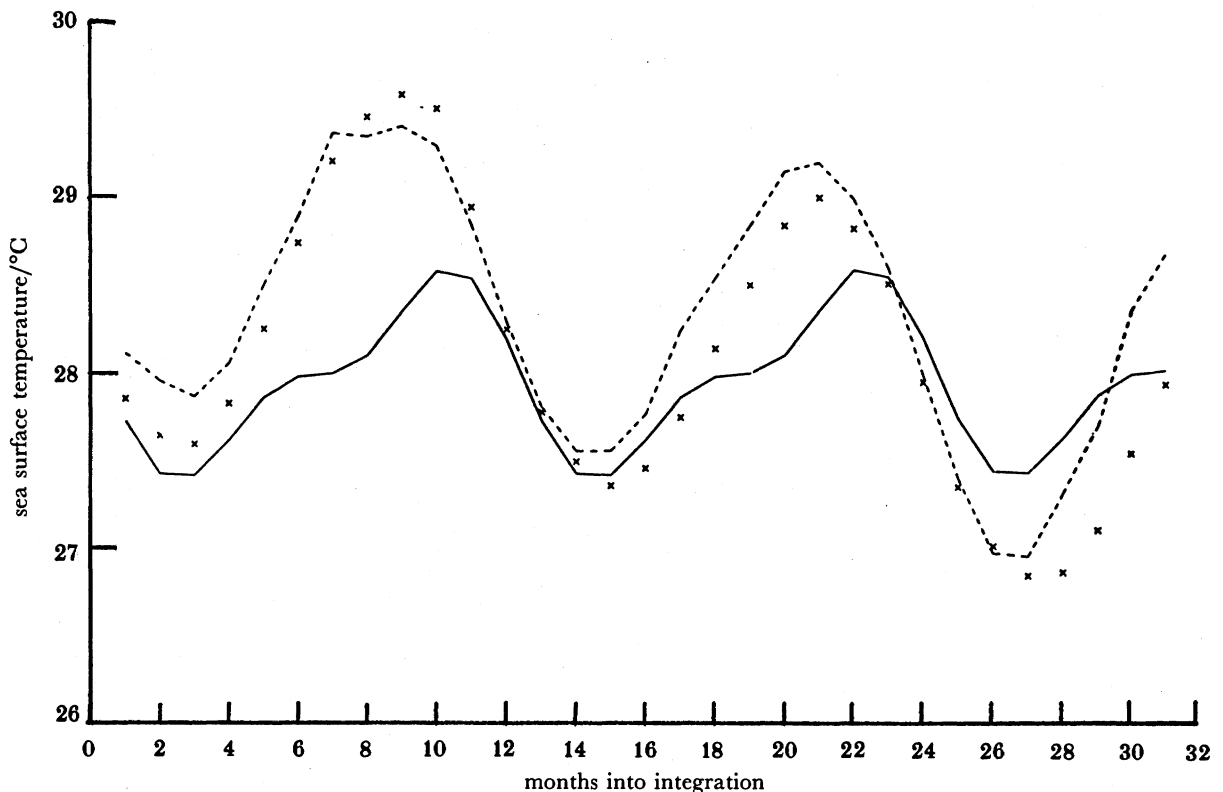


FIGURE 5. The SST evolution for the 31 months of the coupled experiment averaged over the region 2.5–15° S and 180–135° W from climatology (solid line), the coupled model (broken line) and the one-dimensional mixing model (crosses). The coupled model temperatures are approximately 1 °C too high and the one-dimensional model gives a reasonable fit to the full GCM SST evolution. Month 1 on the abscissa corresponds to the first July.

in the atmosphere, in turn, forces the anomalous upper-level divergent flow in figure 3*b* and low-level wind response in figure 4*b*.

Why does the SST in this region rise above climatology in the coupled model? The net surface heat flux over the region is illustrated in figure 6. The zeroes in net surface heating coincide with the turning points in SST, suggesting that the dominant mechanism in the temperature change is local heating. To check this, a one-dimensional version of the GCM mixing scheme was integrated with the heat and momentum fluxes from the coupled model in this region. The version of the mixing scheme used is almost identical to that in the GCM, the

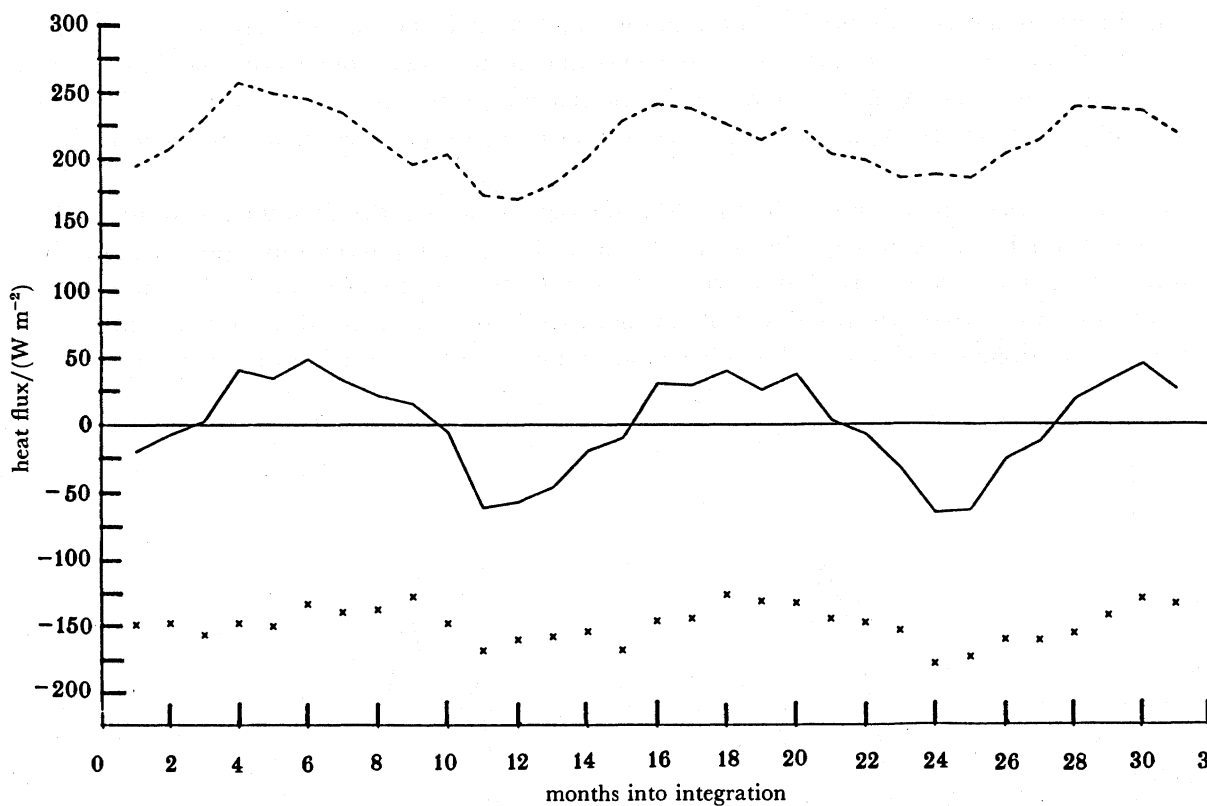


FIGURE 6. The net surface heat flux (solid line), short wave (broken line) and latent heat flux (crosses) components averaged over the region defined in figure 5.

major differences being that only Ekman current shears are included in the calculation of the Richardson number and their salinity effects are not included. Even in the ocean GCM, away from the Equator, only wind-driven Ekman currents contribute significantly to the shear in the mixed layer and so the Ekman approximation is reasonable. (In the later stages of the coupled model experiment, salinity effects may be important as there is a substantial freshening of the surface layers as a consequence of the enhanced precipitation.) The SSTs predicted by the one-dimensional model are also plotted on figure 5 and show a good agreement with those simulated by the coupled GCM. This confirms that the rise in SST in this region is a direct response to the heat flux across the ocean surface. The increase in temperature in this region, compared with climatology, does not necessarily imply that the fluxes are in error (as noted earlier the fluxes are within the climatological estimates) but may also be due to inadequacies

in the ocean model itself (for example, too little vertical diffusion of heat out of the mixed layer).

The dominant components in the net surface heat budget are the short-wave radiative flux and the latent heat flux. These components averaged over the region are also shown in figure 6. The latent heat flux actually decreases slightly over much of the period when the SST is increasing and this is because of a reduction in the local winds that more than compensates the effects of the SST rise (an example of the low-wind region associated with the convergence over the warmest water can be seen in the surface stress field in figure 4*b*). When compared with fluxes from the simulation of the atmospheric model with climatological SSTs (not shown) it is found that the short-wave flux is reduced in the coupled model because of increased cloud. The largest reductions are associated with the maxima in increased convection and have peak values of around  $50 \text{ W m}^{-2}$ . Differences in the net long-wave flux at the ocean surface are generally less than  $10 \text{ W m}^{-2}$  and are therefore of lesser significance in the anomalous heat budget.

To summarize, the ocean in this central Pacific region south of the Equator warms up in the coupled model as a result of local heating. As the SST rises, atmospheric convection increases in intensity and the region is characterized by low-level convergence and light winds. The reduction in low-level winds reduces the evaporative feedback expected from increasing SSTs. Negative feedback by cloud shading effects is also important in reducing the short-wave flux.

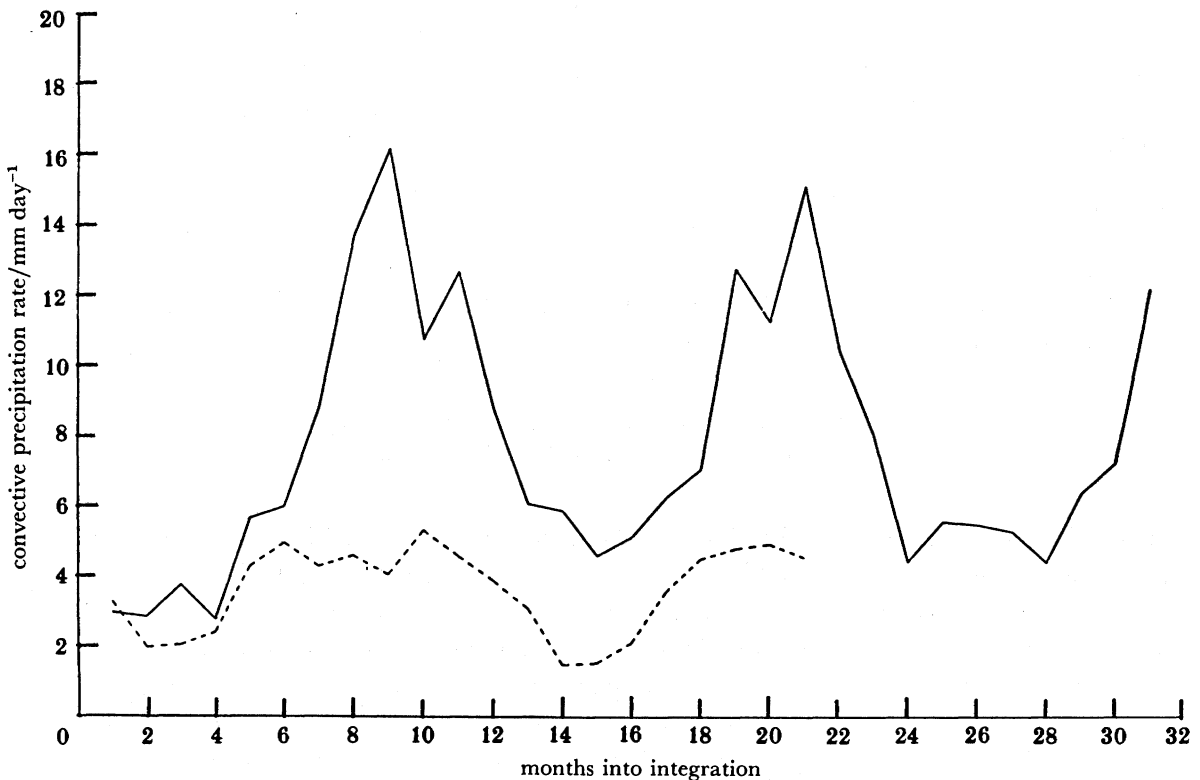


FIGURE 7. The atmospheric model convective precipitation rate in millimetres per day over the region defined in figure 5 from (a) a simulation with climatological seasonally varying SSTs (broken line) and (b) the coupled experiment (solid line). The precipitation rate is considerably larger in the coupled run as a consequence of the increased SSTs. This increased precipitation causes a large anomalous latent heating of the atmosphere in mid-troposphere.

There are large changes in the low-level wind field and the upper-level divergent wind pattern associated with the movement of the main convection zone from the west to the central Pacific. This sequence of events repeats itself each year in the coupled integration.

(b) September

The monthly mean September ssrs from climatology and the last two years of the coupled model are shown in figure 2. Once again the ssrs from each of the years in the coupled model both show the same general differences compared to climatology. In the climatology the warmest water is situated in the west along  $15^{\circ}$  N whereas in the coupled simulation there is

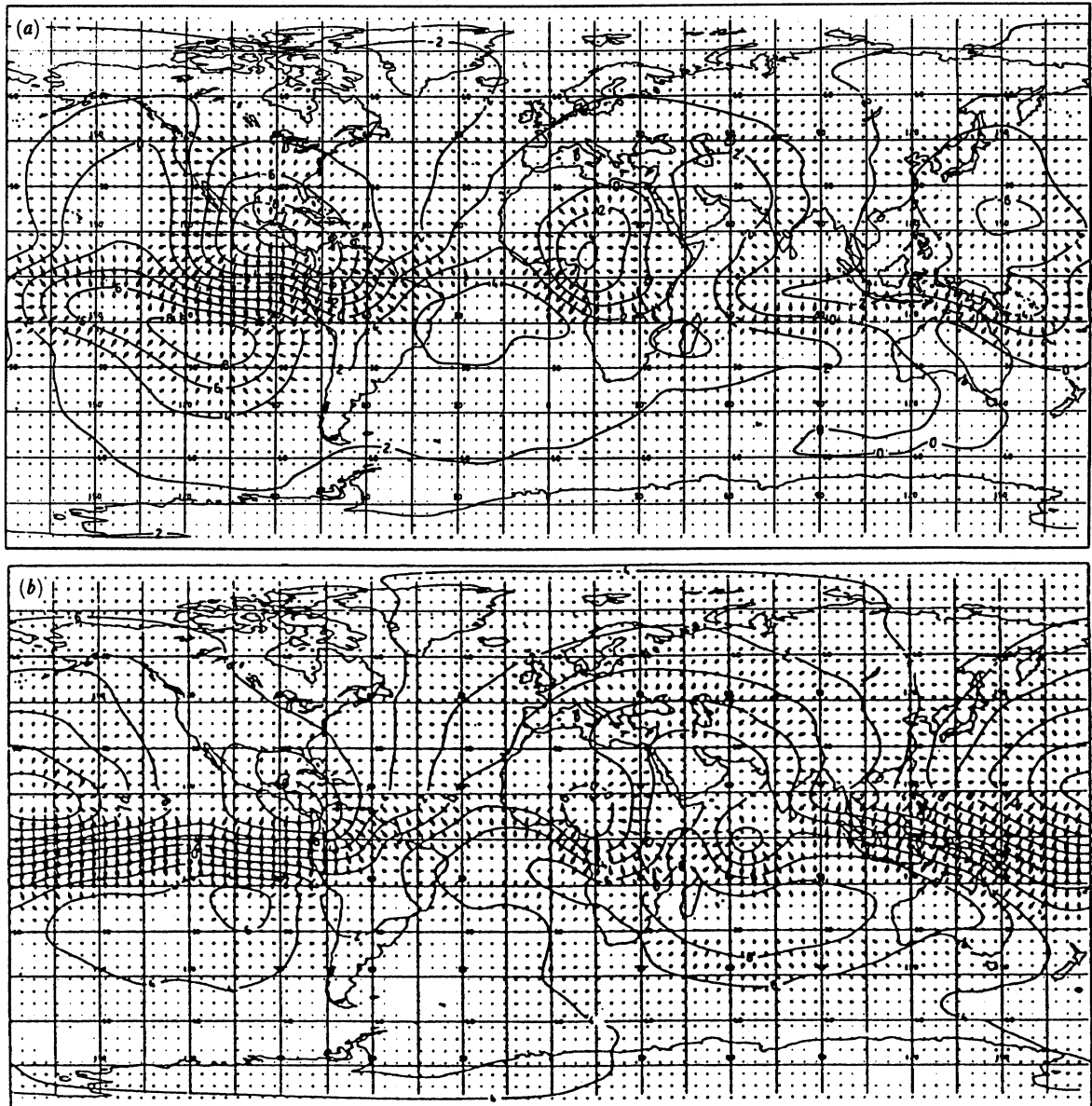


FIGURE 8. The September velocity potential and divergent wind at 250 mbar as simulated by the atmospheric model in (a) a simulation with climatologically varying ssrs and (b) the first year of the coupled experiment. In the coupled model the main forcing region moves from the climatological warm pool (figure 8a) to the ircz east of the dateline.



a local SST maximum along 5–10° N in the central and west Pacific (figure 2*b, c*). In the far east Pacific, simulated temperatures are too warm with the SSTs in each of the model years being similar to each other and different to climatology.

The lack of a west Pacific warm pool in the coupled simulation causes the main atmospheric heating region to be shifted eastwards. This can be seen in the velocity potential and divergent wind fields shown in figure 8*b*. The equivalent field from an atmospheric model integration with climatological SSTs is given in figure 8*a* and shows the local west Pacific maximum in velocity potential located over the climatological warm pool. In the coupled model (figure 8*b*) the maximum shifts eastwards and is located over the new SST maximum east of the dateline. The overall divergent flow pattern in the west and central Pacific is different in the two cases. In the coupled model there is considerably greater divergent meridional flow in the central Pacific than in the uncoupled integration. This raises interesting questions concerning the relative importance of the response of the Hadley and Walker circulations to off-equatorial SST anomalies.

To investigate the cause of the reduction of SSTs in the warm pool region the model temperatures and surface fluxes were averaged over the region covering the warmest water centred on 15° N (this area covers roughly 9–21° N and 142–161° E). Local processes are likely to dominate the warm pool heat budget and to test this hypothesis the one-dimensional mixing model was integrated by using the area-averaged fluxes. Figure 9 shows the time series of SST

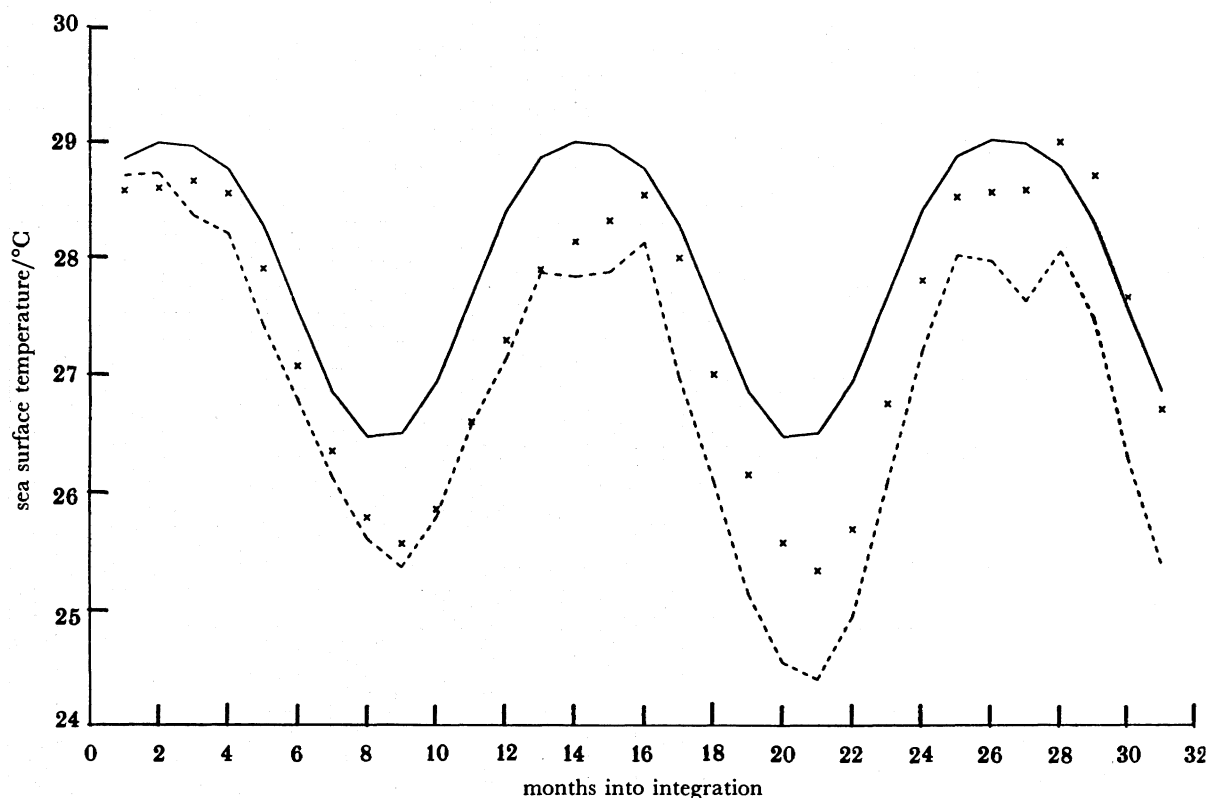


FIGURE 9. As figure 5 but for a region covering 9–21° N and 142–161° E (the region of the climatological warm pool in September). The coupled model temperatures (broken line) are lower than climatology (full line). The one-dimensional model temperatures (crosses) follow closely those from the coupled model over the first year. During the summer months in the coupled model there is a ‘cutting off’ of the temperature cycle.

for this region from climatology, the coupled model and the one-dimensional mixing model. The mixing model captures the cooling of the warm pool indicating the dominance of air-sea heat exchange in the full coupled model. An interesting feature is the 'cutting off' of the coupled model SST cycle from July to October each year (months 13–16 and 25–28 in figure 9). The full extent of this 'cutting off' is not captured by the one-dimensional model. Figure 10*a, b* shows, respectively, the wind stress and its curl from the second August in the coupled simulation. Along 15° N, precisely in the region of the climatologically warmest water, there are large wind stress values and to the north a region of large curl. The large curl generates strong upwelling in the model and therefore cooling of the surface waters. These anomalous winds over the warm pool region are associated with the simulation of the Indian monsoon in the coupled model. Figure 11 shows the August 850 mbar winds over the Indian-Ocean-west-

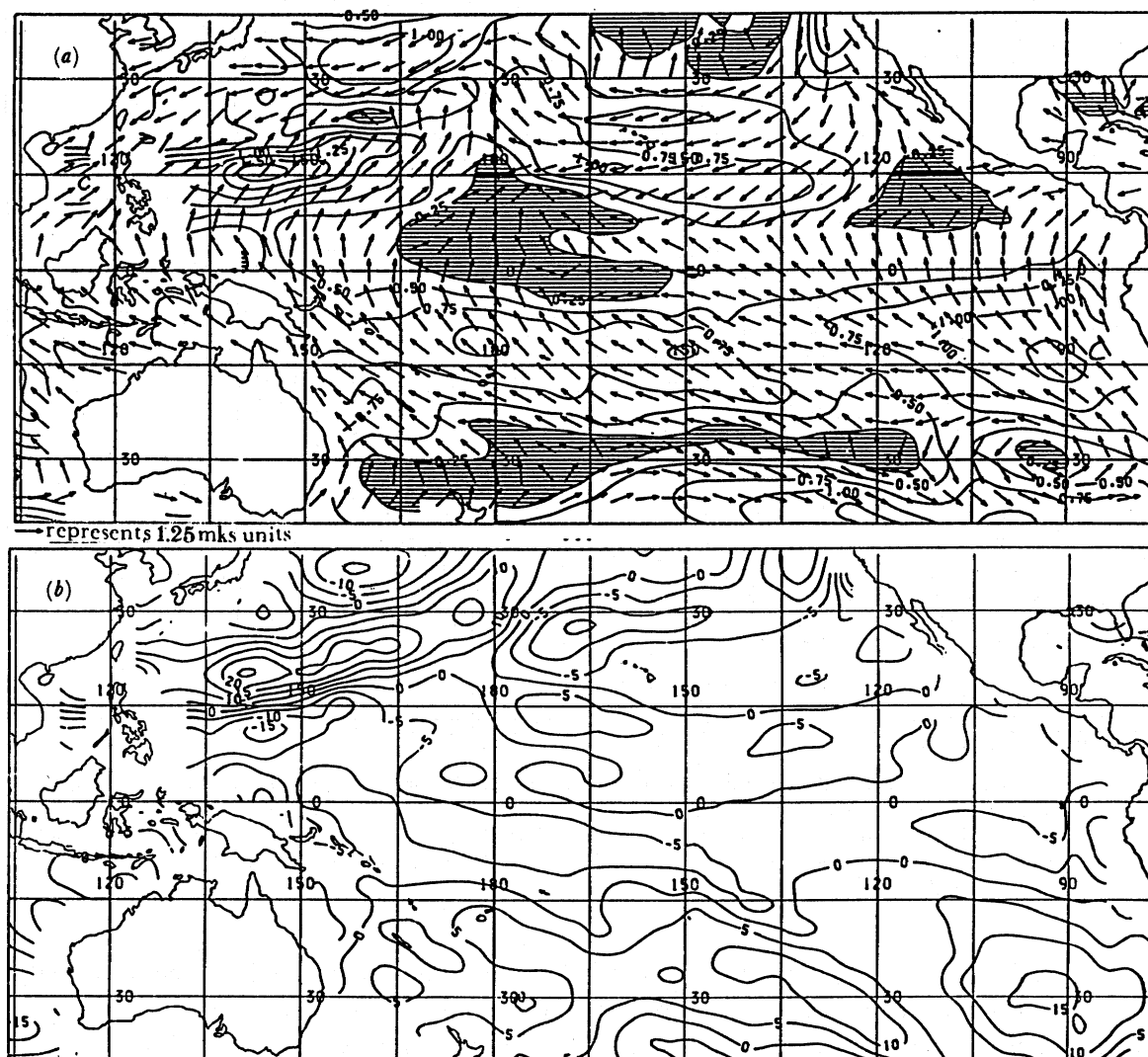


FIGURE 10. The surface wind stress (*a*) and the wind stress curl (*b*) for the month of August from the first year of the coupled model. This August precedes the September in the coupled integration for which the SSTs are shown in figure 2*a*. There are large stresses over the warm pool region centred on 15° N in the west Pacific and these reach peak values of 1.75 dyn cm<sup>-2</sup>. To the north of the high stress area is a region of large wind stress curl (figure 10*b*).

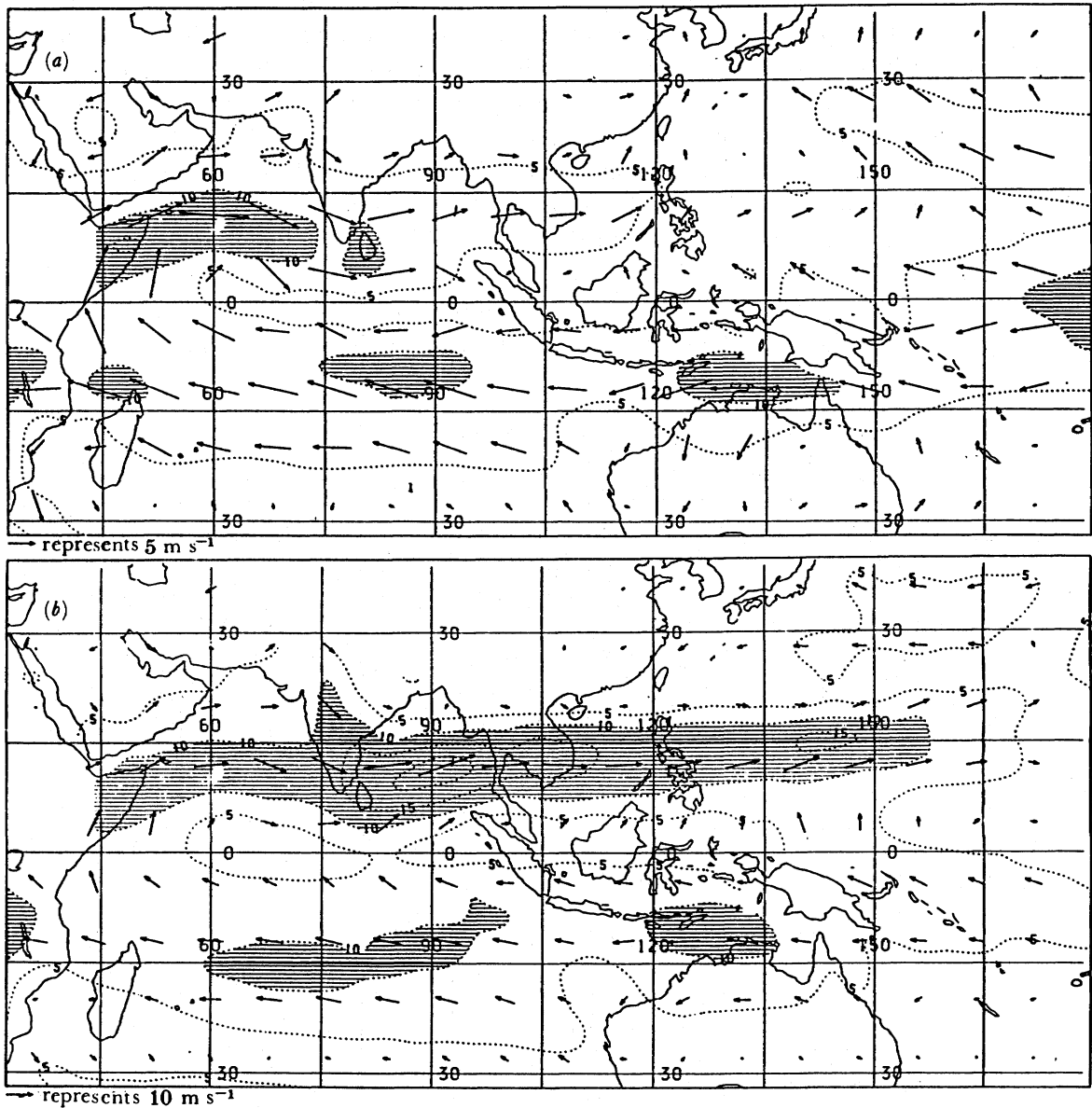


FIGURE 11. The atmospheric model 850 mbar wind vectors and isotachs for August as simulated in (a) a simulation with climatological seasonally varying SSTs and (b) the first year of the coupled integration. In the coupled model the monsoon winds extend across Thailand and into the west Pacific. These anomalous winds lead to the large stresses shown in figure 10. The contour interval is  $5 \text{ m s}^{-1}$  and areas with wind speeds greater than  $10 \text{ m s}^{-1}$  are shaded.

Pacific region from both the coupled model and the atmospheric model integration with climatological SSTs. The monsoon wind pattern shown in figure 11b is repeated during each of the summers in the coupled experiment. Figure 11a shows that with climatological SSTs the atmospheric model does not simulate the eastward extension of the monsoon winds. In reality this extension into the west Pacific does occur on occasions but not each year as in the coupled model. The difference between these two monsoon simulations must be related to the changed heating pattern in the coupled model but the detailed mechanism is not clear.

The other major feature in the September SST simulation is the too-warm water in the east Pacific. This appears to be associated with a weakening of the southeast trades in the coupled model relative to the atmospheric model used alone. In turn, the weakened trades are associated with a reduction in the pressure in the south Pacific high of around 4 mbar. Once again, these changes must be related to the altered heating pattern in the coupled model although the detailed mechanisms require further study. It is noteworthy that although the anomaly appears in the east in the northern summer it essentially disappears by the spring, only to reappear the following summer. The anomaly does not propagate to the west as suggested by the composite picture of Rasmusson & Carpenter (1982).

#### 4. DISCUSSION

In this paper emphasis has been given to the evolution of off-equatorial SSTs in the coupled model. The changes in SST in these regions have been shown to be dominated by local heat exchange across the ocean surface. This is not surprising because these regions are characterized by weak horizontal gradients in SST and by weak winds (and therefore weak currents). Although the SST is simulated to within 1–2 °C of the climatological values there is a large atmospheric response to the altered SST. Where SSTs are in the range 27–30 °C, even small changes in SST can lead to substantial changes in convective activity. This sensitivity is illustrated in figure 12 which shows outgoing long-wave radiation (OLR) plotted against SST for the tropical oceans

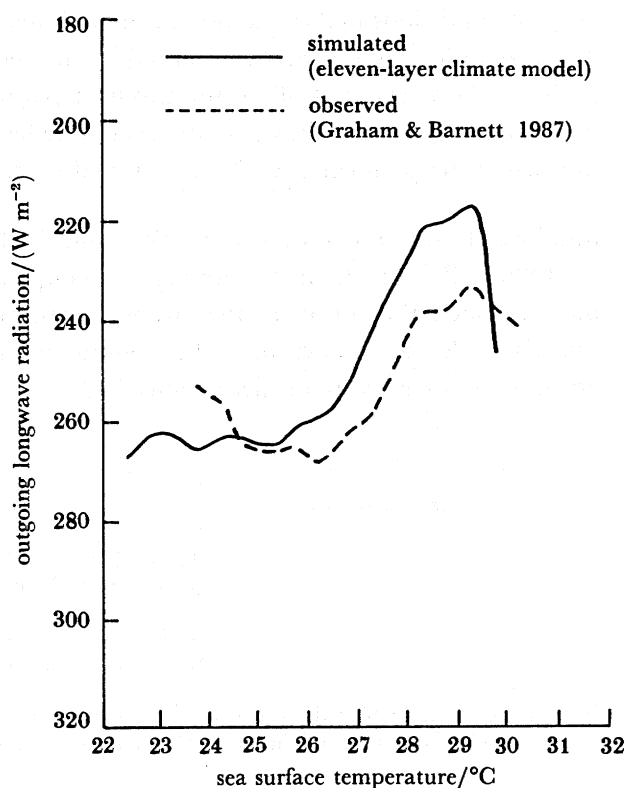


FIGURE 12. Mean OLR fluxes as a function of SST. From both the atmospheric only model and observations the values have been grouped into 0.5 °C bins before plotting. Both curves show the high sensitivity of OLR to SST in the range 27–30 °C. (After Gregory & Rowntree (1989) and Graham & Barnett (1987).)



from observations (Graham & Barnett 1987) and the atmospheric model (Gregory & Rowntree 1989). Although there are differences between the model and data, the rate of change of OLR with SST is essentially the same in both. Above 27 °C there is a rapid decrease of OLR with increasing temperature. These results suggest that in the convergence regions (ITCZ, SPCZ and west Pacific), which overlay the warmest water, accurate modelling of the processes affecting SST is required. This is also evident from the results described in the previous section that also suggest there is a subtle balance between the surface flux components over the warm water regions.

The model was integrated for only  $2\frac{1}{2}$  years and although this is insufficient time to establish a climatology of the coupled model system the results indicate that the model repeats the same systematic 'errors' during each seasonal cycle. Although these are 'errors' in the sense that they recur each year the responses described for both March and September do occur in reality in some years. The air-sea interaction feedbacks described above may well be relevant at these times. It is interesting that there are large changes in the equatorial region of the coupled model, for example the large reduction of the equatorial zonal wind component in the west and central Pacific, causing a decrease in upwelling and that this equatorial response is forced by the off-equatorial anomalies.

If the coupled model integration were continued the model may well oscillate, but around a new climate state similar to that described above. This state exhibits many of the features of a major ENSO event: collapse of easterlies in the west Pacific, warm pool migration eastwards, weakening of the southeast trades and reduction in pressure of the south Pacific high. This similarity of the basic state to ENSO conditions makes the present model unsuitable for detailed ENSO prediction. Continued investigation of the many interactions in the coupled models, combined with good observational data sets, will allow the physical parametrizations to be improved so that the model climate drift can be reduced to an acceptable level for detailed and realistic ENSO simulations/forecasts to be performed with the coupled GCM.

I acknowledge the substantial assistance of members of the Dynamical Climatology Branch at the British Meteorological Office, Bracknell, in developing the coupled TOGA model. In particular, Mike Quinn who performed the coupled integration, Sarah Ineson who helped with the figures and Howard Cattle for a number of useful comments on the manuscript. Thanks also to David Anderson for numerous useful discussions.

#### REFERENCES

- Bottomley, M., Folland, C. K., Hsiung, J., Newell, R. E. & Parker, D. E. 1989 *Global Ocean Surface Temperature Atlas (GOSTA)*. A joint project of the Meteorological Office and the Dept. of Earth, Atmospheric and Planetary Sciences, Massachusetts Institute of Technology. (In the press.)
- Cane, M. A., Zebiak, S. E. & Dolan, S. C. 1986 Experimental forecasts of El Niño. *Nature, Lond.* **321**, 827–832.
- Cox, M. D. 1984 *A primitive equation, 3-dimensional model of the ocean*. GFDL Ocean Group Technical Report No. 1, GFDL/NOAA, Princeton, New Jersey.
- Gordon, C. & Corry, R. A. 1989 A model simulation of the seasonal cycle in the tropical Pacific ocean using climatological and modelled surface forcing. Dynamical Climatology Technical Note. Meteorological Office, Bracknell.
- Graham, N. E. & Barnett, T. P. 1987 Sea surface temperature, surface wind divergence, and convection over tropical oceans. *Science, Wash.* **238**, 657–659.
- Gregory, D. & Rowntree, P. R. 1989 A mass flux convection scheme in use at the UK Meteorological Office. Dynamical Climatology Technical Note. Meteorological Office, Bracknell.

- Mansfield, D. A. & Palmer, T. N. 1986 A study of wintertime circulation anomalies during the past El Niño events using a high resolution general circulation model. I. Influence of model climatology. *Q. Jl R. met. Soc.* **112**, 613–638.
- Pacanowski, R. & Philander, S. G. H. 1981 Parametrization of vertical mixing in numerical models of the tropical oceans. *J. phys. Oceanogr.* **11**, 1443–1451.
- Philander, S. G. H. & Seigel, A. D. 1985 Simulation of El Niño of 1982–1983. In *Coupled ocean-atmosphere models* (ed. J. C. J. Nihoul). Amsterdam: Elsevier.
- Rasmusson, E. & Carpenter, T. 1982 Variations in the tropical sea surface temperature and surface wind fields associated with the Southern Oscillation/El Niño. *Mon. Wea. Rev.* **110**, 354–384.
- Shukla, J. & Blackmon, M. 1986 In *Proceedings of the workshop on comparison of simulations by numerical models of the sensitivity of the atmospheric circulation to sea surface temperature anomalies*, NCAR, Boulder, December 1985. WCP-121.
- Slingo, A., Wilderspin, R. C. & Smith, R. N. B. 1989 The effect of improved physical parametrizations on simulations of cloud and the earth's radiation budget. *J. geophys. Res.* (In the press.)

### Discussion

J. D. NEELIN (*Department of Atmospheric Sciences, University of California, Los Angeles, U.S.A.*). It appears from these results that if Dr Gordon ran his model longer, there would not be much interannual variability, just a strong seasonal cycle. I would just like to note that the very interesting one-dimensional processes that he finds to be important to the seasonal cycle climatology of the coupled system may not be the crucial ones for producing interannual period oscillations. Would Dr Gordon agree with this?

C. GORDON. Yes. The seasonal cycle simulated by the model contains many features that look like ENSO although, as Dr Neelin points out, it is not a true ENSO in the usual sense but rather a climate drift within the model.